



RESEARCH ARTICLE

10.1029/2018MS001494

Key Points:

- Both nonbreaking surface wave and shortwave penetration can enhance the temperature simulation of the upper ocean
- Model improvement due to nonbreaking wave is more considerable than shortwave penetration, especially in subsurface ocean
- The regions where nonbreaking wave generates stronger improvement are where large temperature bias exist

Supporting Information:

- Supporting Information S1

Correspondence to:

F. Qiao,
qiaofl@fio.org.cn

Citation:

Wang, S., Wang, Q., Shu, Q., Scholz, P., Lohmann, G., & Qiao, F. (2019). Improving the upper-ocean temperature in an ocean climate model (FESOM 1.4): Shortwave penetration versus mixing induced by nonbreaking surface waves. *Journal of Advances in Modeling Earth Systems*, 11, 545–557. <https://doi.org/10.1029/2018MS001494>

Received 4 SEP 2018

Accepted 8 FEB 2019

Accepted article online 13 FEB 2019

Published online 27 FEB 2019

Improving the Upper-Ocean Temperature in an Ocean Climate Model (FESOM 1.4): Shortwave Penetration Versus Mixing Induced by Nonbreaking Surface Waves

Shizhu Wang^{1,2} , Qiang Wang³ , Qi Shu^{2,4,5} , Patrick Scholz³ , Gerrit Lohmann³ , and Fangli Qiao^{2,4,5} 

¹College of Oceanic and Atmospheric Sciences, Ocean University of China, Qingdao, China, ²First Institute of Oceanography, Ministry of Natural Resources, Qingdao, China, ³Alfred Wegener Institute Helmholtz Center for Polar and Marine Research (AWI), Bremerhaven, Germany, ⁴Laboratory for Regional Oceanography and Numerical Modeling, Qingdao National Laboratory for Marine Science and Technology, Qingdao, China, ⁵Key Laboratory of Marine Science and Numerical Modeling, Ministry of Natural Resources, Qingdao, China

Abstract As the first mature global ocean general circulation model based on unstructured-mesh methods, the multiresolution Finite Element Sea ice-Ocean Model (FESOM) has shown great capability in reconstructing the ocean and sea ice in both standalone and coupled simulations at a relatively low computational cost. Parameterizations of some important processes, including the vertical mixing induced by surface waves, however, are still missing, contributing to temperature biases in the upper ocean. In this work we incorporate the vertical mixing induced by nonbreaking surface waves derived from a wave model into FESOM and compare its effect with that of shortwave penetration, another key process to vertically redistribute the heat in the upper ocean. Numerical experiments with and without the shortwave penetration scheme and the nonbreaking surface wave mixing reveal that both processes ameliorate the simulation of upper-ocean temperature in middle and low latitudes mainly on the summer hemisphere. The role of nonbreaking surface waves is more pronounced in decreasing the mean cold biases at 50 m (by 1.0 °C, in comparison to 0.5 °C achieved by applying shortwave penetration). We conclude that the incorporation of mixing induced by nonbreaking surface waves into FESOM is practically very helpful and suggest that it needs to be considered in other ocean climate models as well.

Plain Language Summary Nowadays, numerical ocean, weather, and climate forecasts play an important role in the daily life of human beings. An accurate prediction could help us prepare day-to-day activities orderly. However, the prediction ability has been much lower than expected. As an example, ocean models often simulate a warmer sea surface temperature and cooler subsurface (30–100 m deep) temperature in subtropical oceans, especially in summer, which can lead to big errors in the weather and climate forecasting. This situation was partly alleviated by distributing solar radiation in the upper ocean rather than only heating up the ocean surface. Although shortwave penetration makes some improvement on ocean model performance, it is still far from solving the common simulated temperature bias in the upper ocean. The simulated temperature is considerably improved by incorporating the mixing induced by nonbreaking surface waves into the new generation ocean model FESOM. It turns out that the nonbreaking wave is more capable in ameliorating the simulated upper-ocean temperature than the shortwave penetration.

1. Introduction

Numerical models have been widely utilized to reconstruct the climate of the past, to simulate the climate of the present day, and to project the climate in the near future. Regular structured-mesh models, characterized by their easy grid generations and their convenient approach for the discretization of the governing equation, are the first type of models that were developed for climate research. Since the 1950s, when a highly simplified numerical model was first introduced for weather forecasting (Charney et al., 1950), this kind of models are standardly used with different spatial scales (from global to mesoscale) and with different climate backgrounds (from paleo, modern, to future scenarios).

©2019. The Authors.

This is an open access article under the terms of the Creative Commons Attribution-NonCommercial-NoDerivs License, which permits use and distribution in any medium, provided the original work is properly cited, the use is non-commercial and no modifications or adaptations are made.

There are many small geometrical features in the ocean which affect the large-scale ocean general circulation and even the global climate, such as the narrow straits for the Indonesian Throughflow, the small ocean cavities under ice shelves around the Antarctic, and the steep continental slopes along which important ocean currents flow. Also, there are several key regions with critical ocean processes that can impact the large-scale ocean circulation, such as the regions of the western boundary currents and the regions of deep water formation. To adequately resolve these features and key regions, mesh resolutions are required to be much higher than that are currently affordable in long-term simulations of global climate models. This promoted the development of unstructured-mesh ocean models in the past decades (e.g., Blaise et al., 2010; C. Chen et al., 2003; Danilov et al., 2004; Ford et al., 2004; Q. Wang et al., 2008; White et al., 2008). The Finite Element Sea ice-Ocean Model (FESOM), unlike most of the unstructured-mesh ocean models that are intended for coastal and regional applications, is the first mature global unstructured-mesh ocean model that was developed mainly for the purpose of climate research (Danilov et al., 2004; Sidorenko et al., 2011; Timmermann et al., 2012; Q. Wang et al., 2008). It has been assessed for various applications (e.g., Scholz et al., 2013; Q. Wang et al., 2012, 2018) and used as the ocean sea-ice component of the coupled AWI climate model (Rackow et al., 2016; Sidorenko et al., 2015).

With unstructured meshes, horizontal model resolution can be varied conveniently, thus allowing for seamless multiresolution simulations. Global ocean simulations on unstructured meshes with local refinement in regions of small geometrical features have been successfully applied in different studies (e.g., Timmermann et al., 2012; Wekerle et al., 2013). Compared to the traditional two-way nesting techniques used by structured-mesh models, the unstructured meshes of FESOM show great convenience. Local mesh refinement can be realized easily, even in many different regions simultaneously, and the required work is mainly to design meshes with refinement in physically meaningful regions. For example, we can use high resolution in a chosen ocean basin in an otherwise coarse global ocean (Q. Wang et al., 2016; Wekerle, Wang, Danilov, et al., 2017; Wekerle, Wang, von Appen, et al., 2017) or vary the resolution continuously in a global model according to the strength of local eddy variability (Biastoch et al., 2018; Sein et al., 2016) or local Rossby radius (Sein et al., 2017).

Despite the success of ocean models in climate research during the past decades, the development of different numerical and physical aspects of ocean models is an ongoing process (Griffies et al., 2009). Different vertical mixing schemes have been proposed for ocean models, including the Pacanowski and Philander (1981) scheme (PP), the Mellor-Yamada scheme (Mellor & Yamada, 1982), and the K-profile parameterization (KPP; Large et al., 1994), which are widely used in ocean models. A common problem in ocean models using these schemes is the underestimation of the downward heat transport in the upper ocean, especially in summer (Martin, 1985; Mellor, 2001), even after high-frequency winds are incorporated (Ezer, 2000). Artificially exaggerating the vertical mixing coefficients regardless of the real physical processes may result in unrealistic simulation results, that is, improving regional simulations while deteriorating other parts of the global ocean (C. Wang et al., 2014).

In the real ocean, shortwave penetration (SWP) is one of the processes facilitating vertical heat distribution. Influenced by the concentrations of local particulate and dissolved organic matter, such as phytoplankton pigments (Siegel et al., 1995), the ultraviolet and visible portion of the solar radiation can penetrate to a significant degree below the upper mixed layer (Lewis et al., 1990), reaching depths that vary from less than 10 m to more than 100 m (Griffies et al., 2004). Given the important role that SWP plays in redistributing solar heating and decreasing the warm sea surface temperature (SST) bias, it has become a standard implementation in most of the ocean and climate models. The dependence of SWP on the concentration of chlorophyll has been implemented in FESOM (Q. Wang et al., 2014) as suggested by Sweeney et al. (2005), with the optical model of Morel and Antoine (1994).

Another process that enables vertical mixing of heat are nonbreaking surface waves (NBW). Unlike the breaking wave, of which the concomitant turbulent mixing is constrained in the upper few meters (Kantha & Clayson, 2004), the vertical mixing generated by NBW can reach beyond 100-m depth, penetrating through the thermocline into the subthermocline ocean (Babanin & Haus, 2009; D. Dai et al., 2010; Qiao et al., 2004). In order to account for the mixing induced by NBW in Ocean General Circulation Models, NBW is analytically expressed as the function of wave number spectrum which can be calculated using the output of surface wave numerical models, such as the MASNUM wave model (the MARine Science and NUmerical

Table 1
Experiment Setups of Four Finite Element Sea Ice-Ocean Model Simulations

Experiment ID	Shortwave penetration	Nonbreaking surface wave
Ectrl	No	No
Enbw	No	Yes
Eswp	Yes	No
Es&n	Yes	Yes

Note. Ectrl is the control run, where neither shortwave penetration nor nonbreaking surface wave is implemented.

Modeling surface wave model; Qiao et al., 2004). The MASNUM wave model solves the wave energy spectrum balance equation and its characteristic equations in spherical coordinates and then provides B_v , the wave mixing coefficients which can be added to the turbulent mixing coefficients created by standard closure schemes such as Mellor-Yamada, Pacanowski and Philander, and KPP (see also Qiao et al., 2004; supporting information Text S1). NBW can dramatically improve the performance of ocean circulation models for global ocean (Qiao et al., 2010; Shu et al., 2011; Y. Wang et al., 2010), coastal ocean (Lin et al., 2006), and even in lake simulations. Moreover, to simulate the upper ocean, models excluding

traditional turbulence closure schemes could work quite well while only NBW is implemented (Qiao & Huang, 2012). Numerical experiments have shown that the mixing induced by NBW can decrease simulated tropical SST bias (Z. Song et al., 2012b), improve the representation of mixed layer depth (Fan & Griffies, 2014), and lead to more realistic prediction of South Asian summer monsoon system (Y. Song et al., 2012a) in climate models.

This paper presents the improvement of the upper-ocean temperature in FESOM simulations by adding the vertical mixing induced by NBW which is simulated by the MASNUM wave model. The impact of the mixing scheme will be described, which can serve as a reference for future applications. In addition, the effect of NBW is compared to the effect of SWP. The paper is organized as the following. The experimental setup is presented in section 2. The simulation results with and without SWP/NBW are presented in section 3, followed by discussions (section 4) and conclusions (section 5).

2. Experimental Setup

In this study we use FESOM1.4 described by Q. Wang et al. (2014) which is run in a global mesh with a nominal resolution of about 1° in most parts of the ocean, a refinement to about 24-km north of 50°N , and $1/3^\circ$ in the equatorial band, as well as moderate refinement ($1/3^\circ$ to $1/2^\circ$) along the coasts. In the vertical, 47 z-levels are used with a resolution of 10 m in the top 100 m and gradually increased downward. This grid has been used in the previous Coordinated Ocean-ice Reference Experiments phase 2 (CORE II) model intercomparison project (e.g., Q. Wang et al., 2016). We apply the Redi (1982) diffusion and the Gent-McWilliams parameterization (Gent & McWilliams, 1990) in the tracer equations. For vertical mixing, the KPP (Large et al., 1994) is employed.

The model is forced from the surface with the data from CORE II (Large & Yeager, 2009), which includes surface air temperature, specific humidity, surface wind speed, radiation flux, and precipitation. The surface forcing for the river runoff is taken from the interannual monthly data set provided by A. Dai et al. (2009). The ocean is initialized with temperature and salinity fields from the Polar Science Center Hydrographic Climatology v.3 (Steele et al., 2001), and sea ice is initialized with climatological fields obtained from a previous simulation. Four cycles of integration from 1948 to 2009 are carried out sequentially for each numerical experiment. The period 1955–2004 of the last simulation cycle is used in the following analysis.

We carried out four experiments with details of the setups explained in Table 1. The only difference among the simulations is whether SWP or/and NBW are considered. The horizontal resolution of the MASNUM wave model is 0.5° by 0.5° and is forced by QuikSCAT 10-m wind (<https://climatedataguide.ucar.edu/climate-data/quikscat-near-sea-surface-wind-speed-and-direction>) in the period from 1999 to 2009 to get climatologically monthly mean wave-mixing coefficients offline. Then the coefficients are interpolated to the FESOM grid points and added to the mixing coefficients of the KPP scheme in simulations in which the effect of NBW is incorporated. In this study we focus on the wave effects between 80°S and 65°N ; therefore, only the mixing coefficients in this latitudinal range are added.

3. Results

We first investigate the model results in February to explore the impact of SWP and NBW in austral summer. Figure 1 presents the modeled temperature anomalies at 50-m depth for the Ectrl experiment with respect to the World Ocean Atlas 2013 version 2 (WOA13 V2; Locarnini et al., 2013; Figure 1a), as well as for the experiments Enbw, Eswp, and Es&n with respect to Ectrl (Figures 1b–1d). Compared to the WOA13 V2, the Ectrl

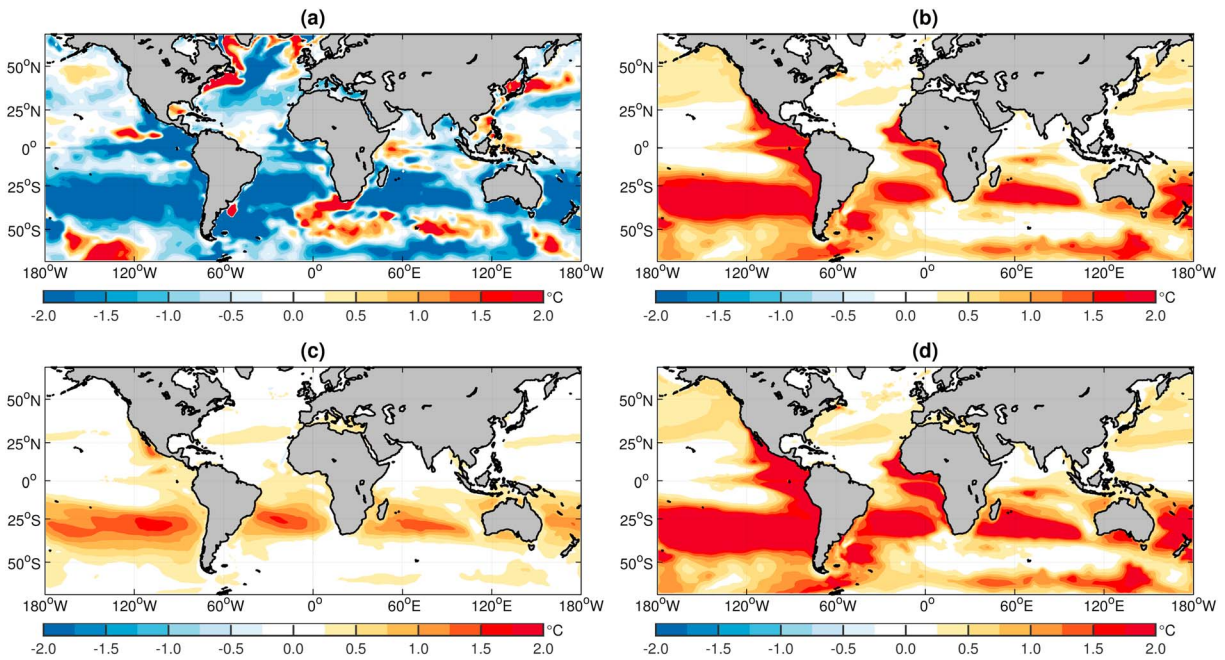


Figure 1. Temperature difference ($^{\circ}\text{C}$) at 50-m depth in February. (a) Ectrl minus World Ocean Atlas 2013 version 2 climatology, (b) Enbw minus Ectrl, (c) Eswp minus Ectrl, and (d) Es&n minus Ectrl.

experiment shows positive temperature biases in a few small regions (mainly in some regions of the Southern Ocean and along the western boundary currents), whereas negative temperature biases dominate in large parts of the world ocean, mostly pronounced in the subtropical region of the Southern Hemisphere (SH) (Figure 1a). Both SWP and NBW tend to warm the ocean at the subsurface where Ectrl shows cold biases (Figures 1b and 1c). The Enbw and the Eswp runs reveal positive temperature anomalies with respect to the control run in a zonal band around 25°S as well as in the eastern tropical Pacific and Atlantic. The warming anomalies in Enbw with a maximum of $\sim 2.0^{\circ}\text{C}$ are almost twice as strong as the warming anomalies of the Eswp run. In addition, warming anomalies in Enbw (Figure 1b) in the Southern Ocean which barely exist in Eswp (Figure 1c) also help to reduce the bias toward the WOA13 V2. Given the large difference in the effects of SWP and NBW, the Es&n simulation largely resembles Enbw (Figures 1b and 1d).

The warming effects of SWP and NBW can reach as deep as 100 m (Figure 2). The cold bias in the subtropics on the SH in the control run is smaller at 100-m depth than at 50-m depth. Accordingly, the warming effect of SWP and NBW in this region becomes smaller with depth. On the Northern Hemisphere, SWP and NBW also reduce the cold biases in the midlatitudes. There are two main findings based on the comparison of different simulations and the observations. It is interesting to see that the locations of pronounced SWP-induced and NBW-induced warming overlap with some of the regions of large cold biases, in particular in the southern subtropics and the eastern tropical Pacific and Atlantic (Figures 1 and 2), effectively reducing the subsurface cold biases (Figures S1 and S2). It is also obvious that NBW has a stronger impact in reducing the cold biases than SWP.

At the surface, the control simulation has large SST biases in a few regions, including the cold biases in the subpolar North Atlantic and the warm biases in the Gulf Stream and Kuroshio regions and along the Antarctic Circumpolar Current (Figure 3a). Previous studies suggested that these biases are associated with poorly resolved mesoscale eddies in coarse-resolution models (e.g., Sein et al., 2016). Indeed, because the source of these biases is not related to the mixing effect of SWP and NBW, applying them does not produce temperature anomaly that can help to reduce these biases (Figures 3b and 3c). As a result of vertical redistribution of heat, SWP and NBW induce negative temperature anomalies at the surface around 30°S on the SH (Figure 3), where they produce positive temperature anomalies at the subsurface (Figures 1 and 2).

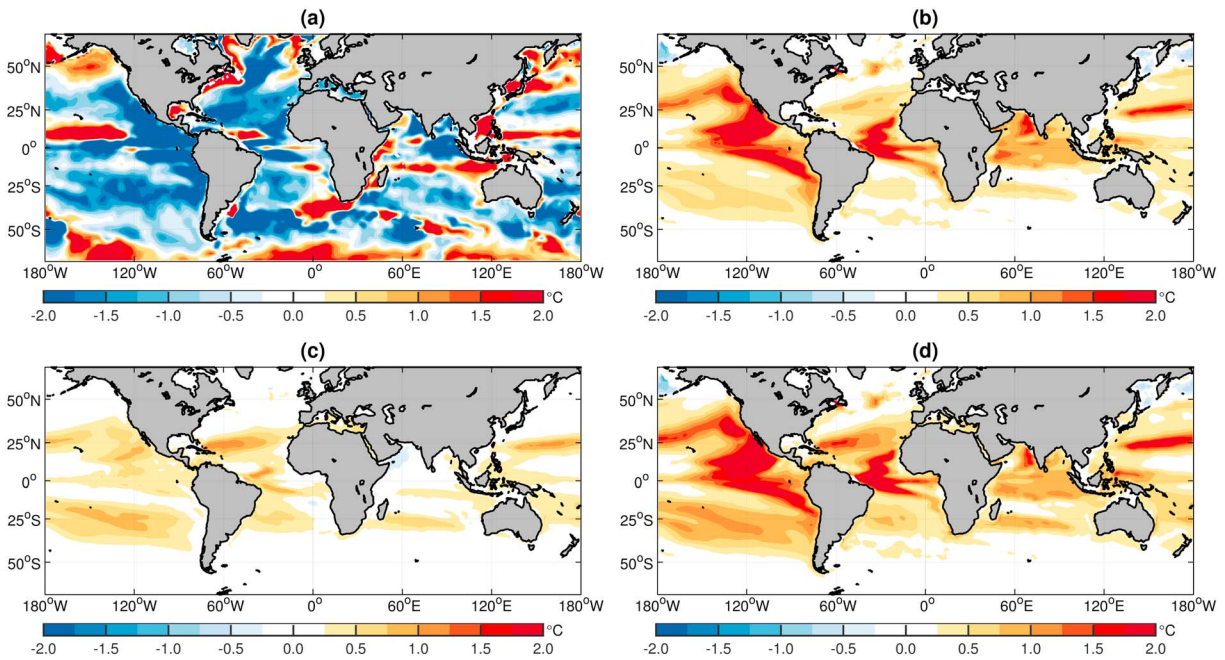


Figure 2. Same as Figure 1 but for the depth of 100 m.

We also need to point out that there are some small regions in the SH where NBW deteriorates the modeled SSTs compared to the WOA13 V2 (Figure S3). Also, for the subsurface, while including NBW improves most of the midlatitude oceans in the summer hemisphere, it slightly deteriorates the small regions in the southeast tropics. It leads to a too warm subsurface (Figures S1a and S1b) and a too cold surface (Figures S3a and S3b) there. These regions correspond to places of strong coastal upwelling and tropical currents, which can impact the upper-ocean temperature as well. We speculate that the model biases related to ocean circulations in these regions are exacerbated after including the NBW mixing.

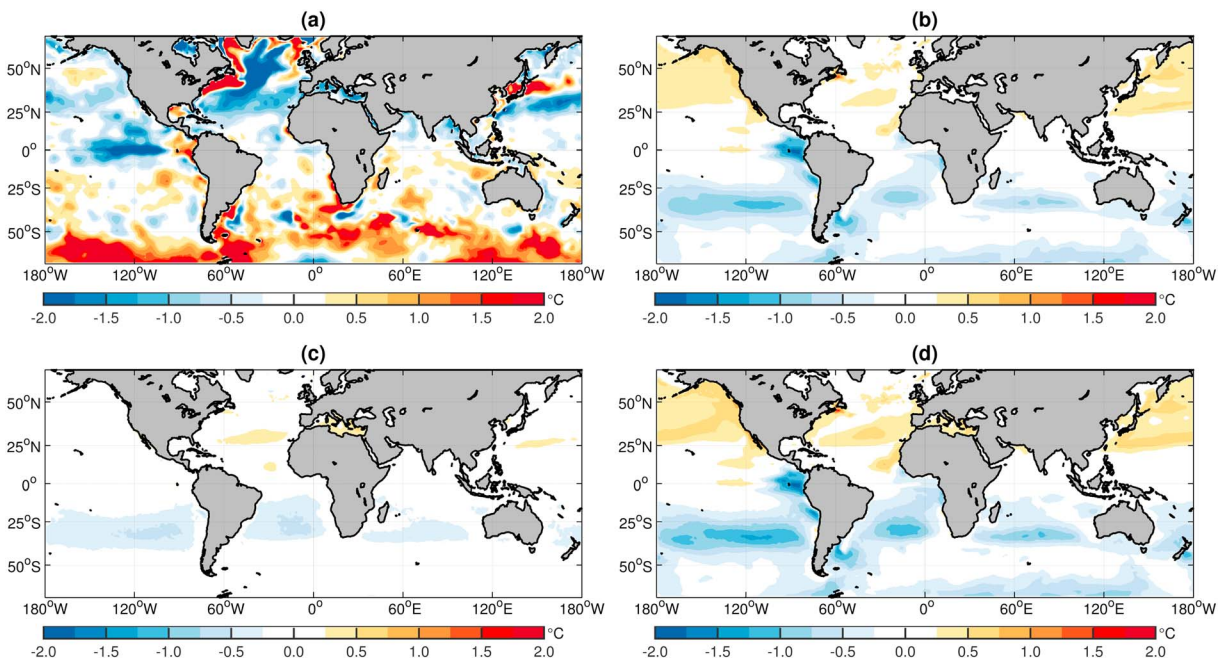


Figure 3. Same as Figure 1 but for the ocean surface.

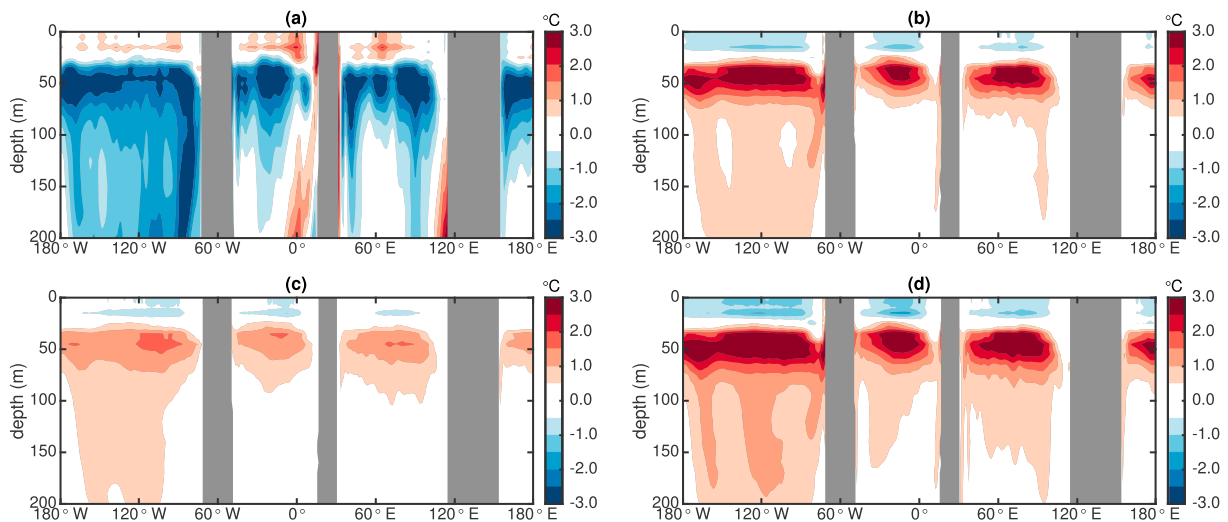


Figure 4. Temperature difference along 30° S (longitude vs. depth) in February. (a) Ectrl minus World Ocean Atlas 2013 version 2 climatology, (b) Enbw minus Ectrl, (c) Eswp minus Ectrl, and (d) Es&n minus Ectrl.

The interaction between mixing and ocean transport processes in these regions needs to be examined in dedicated process studies in future work.

Actually, the strong effect of NBW in the eastern tropical Pacific is unexpected. Within the “Doldrums” where winds are calm or even disappear, the wave-induced mixing should have been negligible, but on the contrary, NBW decreases negative subsurface temperature biases and positive SST biases in this region by up to 2 °C (Figures 1b, 2b, and 3b). We will come back to this in section 4.

Overall, the effects of SWP and NBW significantly improve the simulation, which is better illustrated by the temperature zonal section along 30° S for February (Figures 4 and S4). Compared to the WOA13 V2 climatology, the control run simulates a warmer surface layer (upper 20 to 30 m, ~1.0 °C) and a much colder subsurface layer (from about 30 m down to 200 m, up to 3.0 °C) in all the subtropical ocean basins (Figure 4a). Both SWP and NBW are able to largely reduce the horizontal (Figure 1 and 2) and vertical biases (Figures 4b and 4c) of the control run. The warm biases near the surface and the cold biases centering around 50 m are decreased in Enbw and Eswp, with the role of NBW being more significant. By including both schemes, the modeled temperature biases are significantly reduced (Figure S4d). Therefore, despite the small deterioration of modeled SSTs because of NBW in the subtropics on the SH (Figure 3b), the overall temperature biases are considerably reduced.

The model results of February presented above show that SWP and NBW significantly improve the temperature representation on the SH. In August, they improve the model results on the Northern Hemisphere (Figures S5–S10) in the same way. That is, they are more important on the summer hemisphere. The seasonal evolution of the amendment of SWP and NBW to the upper-ocean temperature in the subtropical band is shown by the diagram of zonally averaged temperature biases at 30°S in Figure 5. When these two processes are not included in the model, cold biases exist in the subsurface ocean all year long (Figure 5a): They occupy the whole water column in winter, deepen from spring to fall, and peak in summer. The effects of SWP and NBW in reducing the biases evolve accordingly with time (Figures 5b–5d), following both the strength and location of the biases in the control run (Figure 5a). Consequently, the model simulations are significantly improved when both processes are considered (Figure S11).

4. Discussions

The prominent role of SWP and NBW on the summer hemisphere is related to the seasonal change of water column stratification. In summer, heated surface water of relatively low density generates stable stratification and increases the degree of decoupling between surface and subsurface (Capotondi et al., 2012). Including the extra mixing induced by NBW and the redistribution of solar radiation by SWP can weaken

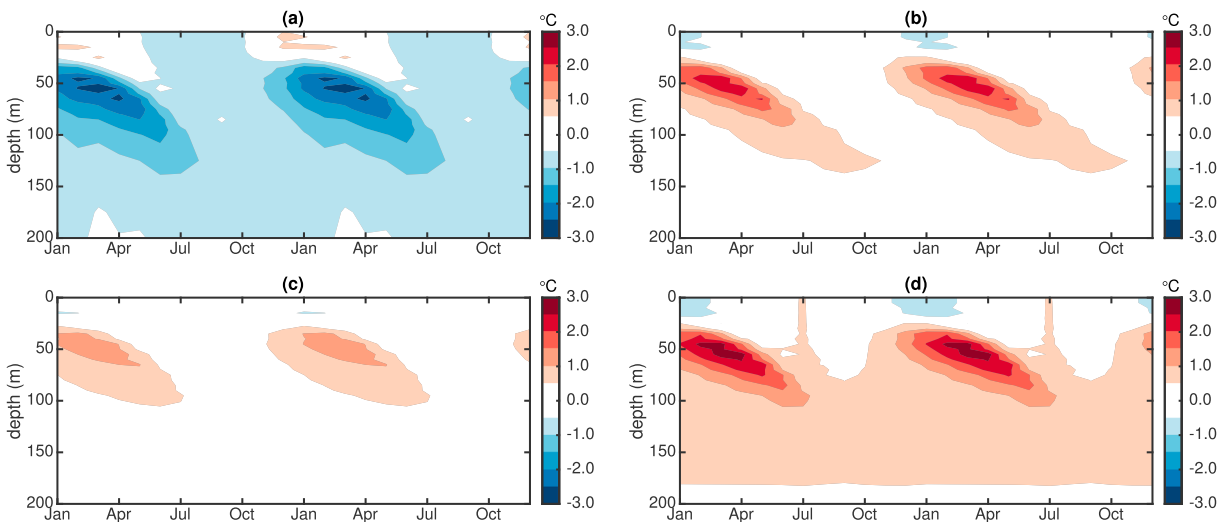


Figure 5. Seasonal evolution of zonal mean temperature difference along 30° S (month vs. depth, in °C). (a) Ectrl minus World Ocean Atlas 2013 version 2 climatology, (b) Enbw minus Ectrl, (c) Eswp minus Ectrl, and (d) Es&n minus Ectrl.

this stratification and produce more reasonable temperature spread in the vertical. In winter, cooling of the surface water reduces the stability, and the vertical mixing provided by the KPP scheme can lead to reasonable subsurface temperature. In this case the effect of SWP and wave mixing becomes secondary, being masked by the vertical mixing induced by strong surface cooling. To qualitatively manifest the cooling effects at surface and the warming effects at subsurface of SWP and NBW on the summer hemisphere, temperature deviations from the WOA13 V2 within the latitudinal band of 60–10°S in February are shown in Figure 6. Overall, temperatures are more biased at subsurface than at surface, given that in the ocean standalone model, ocean surface is directly forced by realistic atmospheric data (in our case, CORE II forcing). Minor positive SST biases (<0.5 °C, inset of Figure 6a) exist in the Ectrl run, which could be slightly but correctly decreased after SWP and NBW are incorporated. Compared with the small positive SST biases, notable negative biases occupy the subsurface layer in Ectrl, with the mean deviations being −1.2 °C at 50 m and −0.5 °C at 100 m. For the two temperature-correction processes, SWP warms the subsurface up and decreases the cold biases to −0.6 °C at 50 m, while NBW decreases the biases to −0.1 °C. We need to notice that the combination of both processes may be so strong at some points that changes the temperature bias from negative to positive (inset of Figure 6b). This can be overcome by multiplying a constant factor with the B_v parameter as suggested by Shu et al. (2011), to weaken the too strong wave-induced mixing. A finer tuning of the NBW scheme by exploring such a factor will be done in our future work. It is important for us that the upper-ocean temperature biases were significantly reduced by applying the current NBW and SWP schemes.

Although the roles of SWP and NBW in improving the temperature simulation on the summer hemisphere are similar, the ways they achieve the improvement are different. SWP serves as a flux term in the energy equation. Most of the temperature improvements are where insolation is strong (i.e., summertime) and the concentration of chlorophyll is low (Figure 7). In these regions, only after the penetration process of shortwave radiation is considered can the excessive solar radiation be redistributed in the vertical. In regions of high upwelling rate (e.g., eastern coasts of the Pacific), the abundant chlorophyll absorbs almost all the solar radiation in the superficial layer, making the role of SWP negligible in these coastal areas compared to NBW (Figures 1–4).

On the other hand, the modification of NBW on temperature depends not only on the mixing coefficient B_v which is a function of wave frequency and wave number (Qiao et al., 2004) but also on the vertical temperature gradient, as the vertical diffusion flux is $F = -B_v \frac{\partial T}{\partial z}$. This can explain why NBW exerts a great impact on water temperature in the eastern tropical Pacific basins. Figure 8 shows the horizontal distribution of B_v , vertical temperature gradients, and the resulting temperature changes in the top layer of FESOM. As expected, mixing coefficients are much smaller in this Doldrum region (Figure 8a) than in the regions of

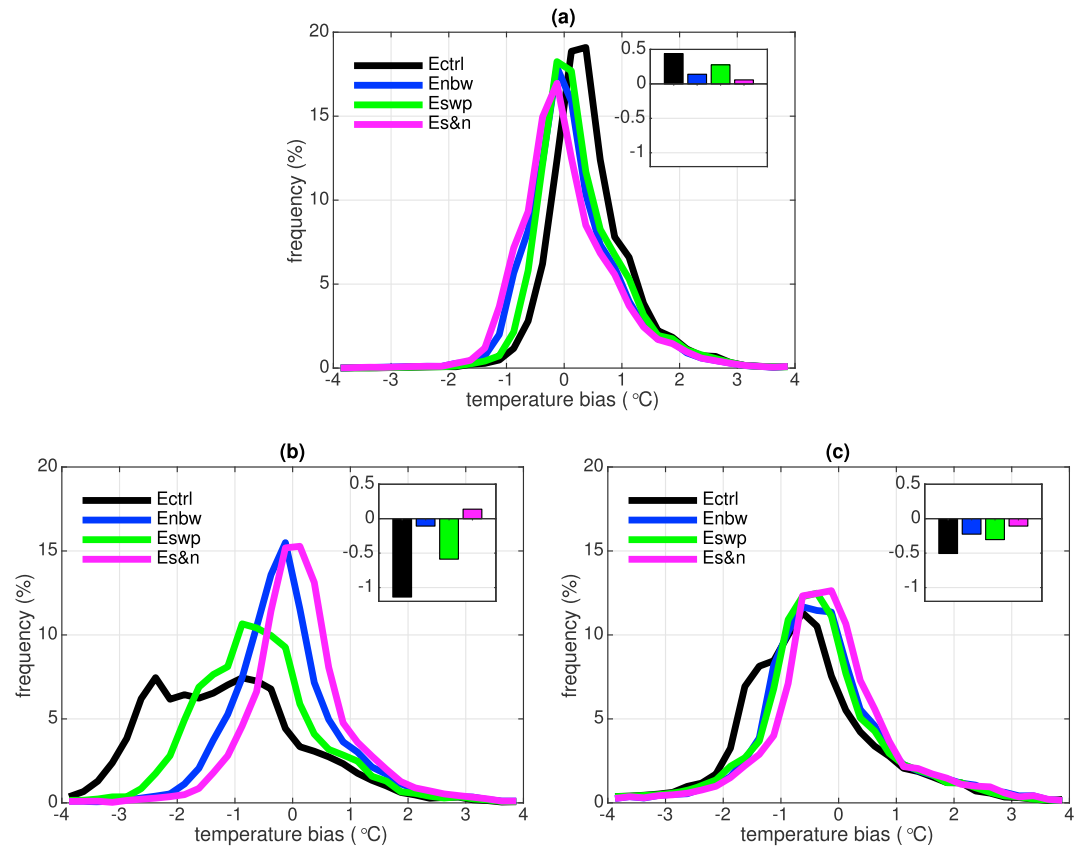


Figure 6. Relative frequency plots of model temperature deviations from the World Ocean Atlas 2013 version 2 in 0.25 °C bins. (a) SST, (b) 50-m depth, and (c) 100-m depth. Considered are temperatures within the band of 60–10° S in February. (inset) Mean temperature deviations from the World Ocean Atlas 2013 version 2.

strong westerlies. However, the shallow mixed layer and the stable stratification form a large vertical temperature gradient in the top layer (Figure 8b), resulting in remarkable temperature changes (Figure 8c). It is noteworthy that the inclusion of SWP and NBW does not decrease the simulated temperature biases in the northwest corner of the North Atlantic and along the western boundary currents (including the Kuroshio and Gulf Stream; Figures 1–3 and S1–S10). It has been shown that using eddy-resolving resolution

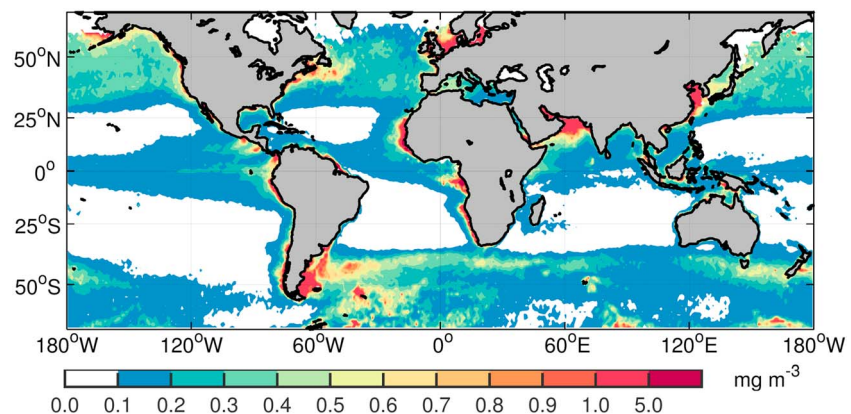


Figure 7. Monthly chlorophyll concentration climatology (1997–2010) in February. The data are found online (<https://oceancolor.gsfc.nasa.gov/>).

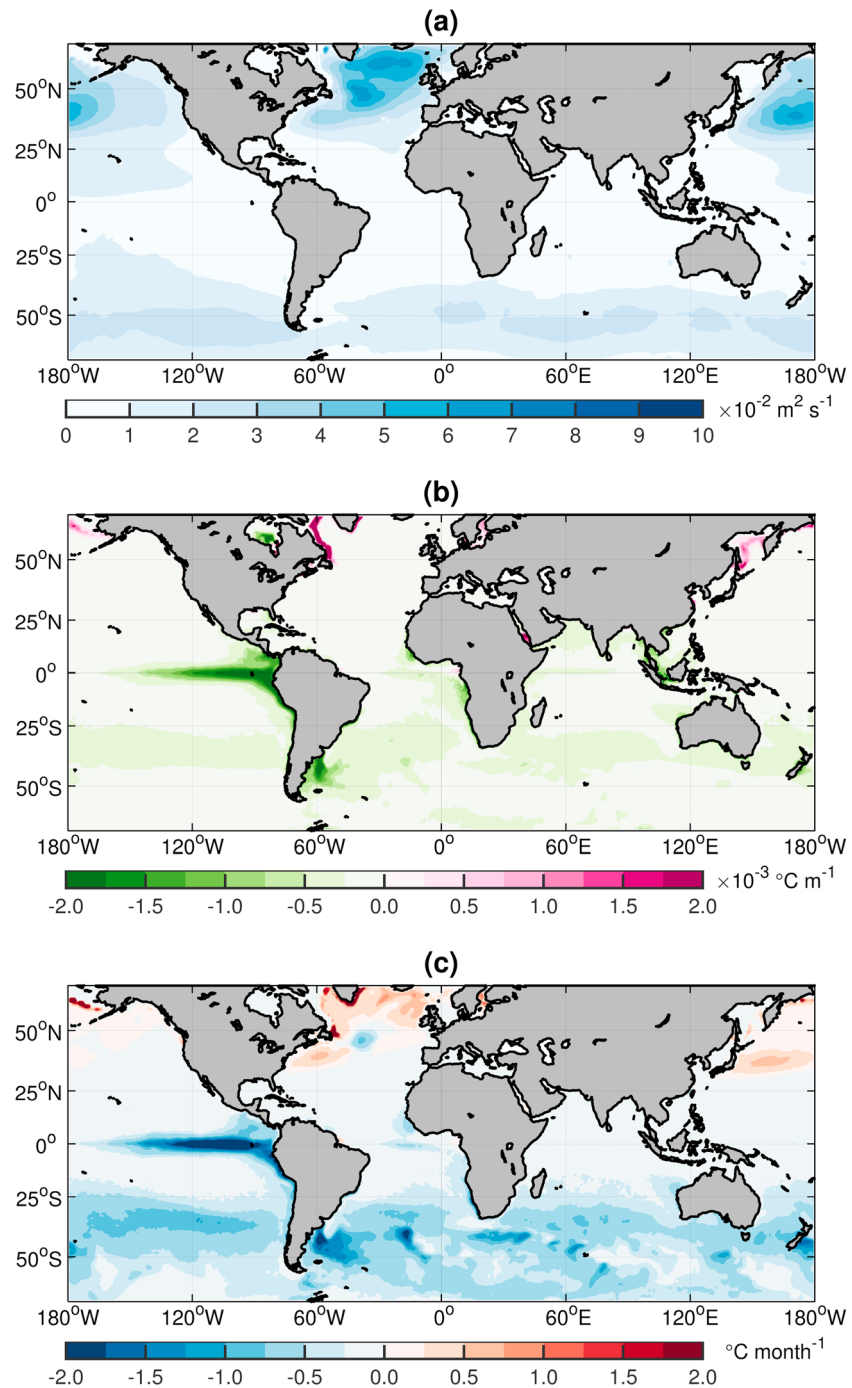


Figure 8. Horizontal spreads of (a) nonbreaking wave-induced mixing coefficients, (b) vertical temperature gradients, and (c) wave-induced temperature changes of the top layer.

can significantly improve the representation of the ocean dynamics and the air-sea interaction processes in these regions, thus reducing the temperature biases (e.g., Kwon et al., 2010; Ma et al., 2016; Sein et al., 2016). The positive temperature biases in the Southern Ocean around the Antarctica at subsurface waters are not much meliorated by including the NBW-induced mixing (Figures 1–3). These biases are common in ocean climate models of coarse resolution and suggested to be possibly associated with insufficient effect of eddy parameterization (Sallée et al., 2013). Adjustment of the eddy skew diffusivity or using high resolution to explicitly resolve mesoscale eddies is required to reduce these biases in ocean climate models.

Eddy-induced advection can create restratification (Chanut et al., 2008) and diminish the mixed layer depth in the water column. This process may counteract the de-stratification of the vertical mixing due for example to wind-induced wave mixing. Therefore, the performance of temperature simulation in the upper ocean can be impacted by the representation of eddies in the surface boundary layer. For parameterizing near-surface eddy fluxes, in this work we used the scheme described in Danabasoglu et al. (2008) which is a simplified version of the scheme introduced by Ferrari et al. (2008). As was pointed out by Canuto and Dubovikov (2011), however, in this scheme the eddy-induced advection fails to entail restratification in the mixed layer. Actually, improving eddy parameterizations especially for the boundary layers is still an ongoing active research field (Canuto et al., 2018; Ferrari et al., 2010; Gent, 2011). So, if we apply other more appropriate schemes for representing near surface eddy fluxes, the NBW mixing parameterization, presumably, should be adjusted to maintain the good performance in the upper-ocean temperature.

We inspected a FESOM mesoscale-eddy resolving simulation described by Sein et al. (2017). In their model setup, they used a model grid with variable resolution set to half of the local first baroclinic Rossby radius, and the Gent-McWilliams parameterization was switched off for the whole ocean. Resolved eddies show the capability to reduce temperature biases in the northwest corner of the North Atlantic and along the western boundary currents. However, the temperature biases at 50-m depth on the summer hemisphere remain nearly the same as in our coarse-resolution simulation (see Figure S12). This indicates that in these regions the upper-ocean temperature biases, independent on parameterizing or resolving mesoscales in the model, require the NBW-induced mixing (and SWP) to be alleviated. Possibly this could be due to the fact that the NBW mixing parameterization is the more influential factor determining the simulated upper-ocean temperature in summertime than the effects of mesoscale eddies in the mixed layer. In our study we did not apply parameterizations of submesoscale eddies, which can also impose some effects of restratification in the mixed layer. Considering the fact that the NBW and SWP parameterizations together slightly overcorrected the temperature bias (Figure 6b), we speculate that including the effect of submesoscale eddies would compensate the small overcorrection, thus further improving the model performance.

5. Conclusions

In this work the vertical mixing parameterization of NBW was incorporated into the unstructured-mesh ocean model FESOM. The mixing coefficients are provided from the output of the MASNUM wave model. The effect of wave mixing was compared to that of SWP. We demonstrated that both processes have the potential to redistribute heat from surface to subsurface and improve the temperature simulation in the upper ocean. The downward heat transfer decreases the cold biases in the subsurface ocean, especially for the summer hemisphere where stable stratification exists. NBW leads to much stronger improvement on the temperature simulation than SWP. The surface wave-induced mixing also reduces the temperature biases in the eastern tropical Pacific, where strong vertical temperature gradients exist.

As the ocean is the flywheel of the climate system, the better simulation of the upper ocean by including the effect of NBW could improve climate model fidelity, for example, the less-biased mixed layer depth (Fan & Griffies, 2014) and the more realistic prediction of South Asian summer monsoon system (Y. Song et al., 2012a). Recent analysis has shown that climate models taking part in Coupled Model Intercomparison Project Phase 5 (CMIP5) models tend to have too deep surface mixed layers in winter in subtropical regions, which can also be alleviated by including the NBW mixing (S. Chen et al., 2018). Although our analysis in this work is done for one particular ocean model with one particular wave model incorporated, the identified considerable improvement in the upper-ocean temperature clearly indicates the importance of the NBW mixing process, which presumably needs to be considered in other ocean climate models as well.

A limitation of this work is the applied parameterization of near-surface eddy fluxes. The employed scheme may not accurately represent the restratification of mesoscale eddies in the surface mixed layer. However, simulations resolving mesoscale eddies have shown temperature biases in subtropical and tropical upper oceans very similar to those obtained in coarse-resolution models. That is to say, the cold bias in the subsurface layer seems to be a persistent feature independent on whether the mesoscale is resolved or not. Therefore, applying the NBW mixing and SWP parameterizations is suggested to be required in general in ocean climate models. To compare the respective role of NBW and eddies in determining the

upper-ocean temperature in future work, we need to implement in our model version a physically sounder scheme (e.g., Canuto & Dubovikov, 2011) for representing eddy fluxes in the mixed layer and use eddy-resolving setups as well.

In addition, it remains to see whether the wave-induced mixing can reduce temperature biases in coupled climate models. With sea ice decline in a warming climate, the effect of wave-induced mixing in polar regions should not be neglected in climate simulations. Properly simulating ocean waves in polar regions and taking the relevant wave mixing processes into account are important topics that we need to undertake in future work.

Acknowledgments

The authors thank two anonymous referees whose valuable criticism helped us to improve the integrity of the paper. This research is jointly supported by the NSFC-Shandong Joint Fund for Marine Science Research Centers (grant U1606405), the international cooperation project of Indo-Pacific ocean environment variation and air-sea interaction (grant GASI-IPOVAI-05), and the International cooperation project on the China-Australia Research Centre for Maritime Engineering of Ministry of Science and Technology, China (grant 2016YFE0101400). Qi Shu is funded by the National Key Research and Development Program of China (grant 2016YFC1401407). Shizhu Wang is funded by China Scholarship Council (CSC). Special thank goes to Dmitry V. Sein who provides us with the FESOM-XR data. We thank Xun Gong for fruitful discussion on the hydrography of the Pacific and Xunqiang Yin for setting up the MASNUM wave model. The free access to different observation data sets and reanalysis data extraordinarily facilitates our work, so their efforts are highly appreciated. MASNUM wave model and the coefficients of vertical mixing induced by nonbreaking waves can be downloaded online (<http://data.fio.org.cn/qiaofl/WSZ-JAMES-2018>). FESOM v1.4 can be downloaded online (https://swrep01.awi.de/projects/fesom/after_registration). Mesh partitioning in FESOM is based on a METIS version 5.1.0 package developed at the Department of Computer Science and Engineering at the University of Minnesota (<http://glaros.dtc.umn.edu/gkhome/views/metis>). METIS and the solver pARMS (Li et al., 2003) present separate libraries which are freely available subject to their licenses. The simulation results used in this paper can be obtained from the authors upon request. The authors declare that they have no conflict of interest.

References

- Babanin, A. V., & Haus, B. K. (2009). On the existence of water turbulence induced by nonbreaking surface waves. *Journal of Physical Oceanography*, *39*(10), 2675–2679. <https://doi.org/10.1175/2009JPO4202.1>
- Biaostoch, A., Sein, D., Durgadoo, J. V., Wang, Q., & Danilov, S. (2018). Simulating the Agulhas system in global ocean models—nesting vs. multi-resolution unstructured meshes. *Ocean Modelling*, *121*, 117–131. <https://doi.org/10.1016/j.ocemod.2017.12.002>
- Blaise, S., Comblen, R., Legat, V., Remacle, J.-F., Deleersnijder, E., & Lambrechts, J. (2010). A discontinuous finite element baroclinic marine model on unstructured prismatic meshes. *Ocean Dynamics*, *60*(6), 1371–1393. <https://doi.org/10.1007/s10236-010-0358-3>
- Canuto, V., Cheng, Y., Dubovikov, M., Howard, A., & Leboissetier, A. (2018). Parameterization of mixed layer and deep-ocean mesoscales including nonlinearity. *Journal of Physical Oceanography*, *48*(3), 555–572. <https://doi.org/10.1175/JPO-D-16-0255.1>
- Canuto, V., & Dubovikov, M. (2011). Comparison of four mixed layer mesoscale parameterizations and the equation for an arbitrary tracer. *Ocean Modelling*, *39*(1–2), 200–207. <https://doi.org/10.1016/j.ocemod.2011.04.008>
- Capotondi, A., Alexander, M. A., Bond, N. A., Curchitser, E. N., & Scott, J. D. (2012). Enhanced upper ocean stratification with climate change in the CMIP3 models. *Journal of Geophysical Research*, *117*, C04031. <https://doi.org/10.1029/2011JC007409>
- Chanut, J., Barnier, B., Large, W., Debreu, L., Penduff, T., Molines, J. M., & Mathiot, P. (2008). Mesoscale eddies in the Labrador Sea and their contribution to convection and restratification. *Journal of Physical Oceanography*, *38*(8), 1617–1643. <https://doi.org/10.1175/2008JPO3485.1>
- Charney, J. G., Fjörtoft, R., & Neumann, J. v. (1950). Numerical integration of the barotropic vorticity equation. *Tellus*, *2*(4), 237–254.
- Chen, C., Liu, H., & Beardsley, R. C. (2003). An unstructured grid, finite-volume, three-dimensional, primitive equations ocean model: Application to coastal ocean and estuaries. *Journal of Atmospheric and Oceanic Technology*, *20*(1), 159–186. [https://doi.org/10.1175/1520-0426\(2003\)020<0159:AUGFVT>2.0.CO;2](https://doi.org/10.1175/1520-0426(2003)020<0159:AUGFVT>2.0.CO;2)
- Chen, S., Qiao, F., Huang, C., & Song, Z. (2018). Effects of the non-breaking surface wave-induced vertical mixing on winter mixed layer depth in subtropical regions. *Journal of Geophysical Research: Oceans*, *123*, 2934–2944. <https://doi.org/10.1002/2017JC013038>
- Dai, A., Qian, T., Trenberth, K. E., & Milliman, J. D. (2009). Changes in continental freshwater discharge from 1948 to 2004. *Journal of Climate*, *22*(10), 2773–2792. <https://doi.org/10.1175/2008JCLI2592.1>
- Dai, D., Qiao, F., Sulisz, W., Han, L., & Babanin, A. (2010). An experiment on the nonbreaking surface-wave-induced vertical mixing. *Journal of Physical Oceanography*, *40*(9), 2180–2188. <https://doi.org/10.1175/2010jpo4378.1>
- Danabasoglu, G., Ferrari, R., & McWilliams, J. C. (2008). Sensitivity of an ocean general circulation model to a parameterization of near-surface eddy fluxes. *Journal of Climate*, *21*(6), 1192–1208. <https://doi.org/10.1175/2007JCLI1508.1>
- Danilov, S., Kivman, G., & Schröter, J. (2004). A finite-element ocean model: Principles and evaluation. *Ocean Modelling*, *6*(2), 125–150. [https://doi.org/10.1016/S1463-5003\(02\)00063-X](https://doi.org/10.1016/S1463-5003(02)00063-X)
- Ezer, T. (2000). On the seasonal mixed layer simulated by a basin-scale ocean model and the Mellor-Yamada turbulence scheme. *Journal of Geophysical Research*, *105*(C7), 16,843–16,855. <https://doi.org/10.1029/2000JC900088>
- Fan, Y., & Griffies, S. M. (2014). Impacts of parameterized Langmuir turbulence and nonbreaking wave mixing in global climate simulations. *Journal of Climate*, *27*(12), 4752–4775. <https://doi.org/10.1175/JCLI-D-13-00583.1>
- Ferrari, R., Griffies, S. M., Nurser, A. G., & Vallis, G. K. (2010). A boundary-value problem for the parameterized mesoscale eddy transport. *Ocean Modelling*, *32*(3–4), 143–156. <https://doi.org/10.1016/j.ocemod.2010.01.004>
- Ferrari, R., McWilliams, J. C., Canuto, V. M., & Dubovikov, M. (2008). Parameterization of eddy fluxes near oceanic boundaries. *Journal of Climate*, *21*(12), 2770–2789. <https://doi.org/10.1175/2007JCLI1510.1>
- Ford, R., Pain, C., Piggott, M., Goddard, A., De Oliveira, C., & Umpleby, A. (2004). A nonhydrostatic finite-element model for three-dimensional stratified oceanic flows. Part I: Model formulation. *Monthly Weather Review*, *132*(12), 2816–2831. <https://doi.org/10.1175/MWR2824.1>
- Gent, P. R. (2011). The Gent-McWilliams parameterization: 20/20 hindsight. *Ocean Modelling*, *39*(1–2), 2–9. <https://doi.org/10.1016/j.ocemod.2010.08.002>
- Gent, P. R., & McWilliams, J. C. (1990). Isopycnal mixing in ocean circulation models. *Journal of Physical Oceanography*, *20*(1), 150–155. [https://doi.org/10.1175/1520-0485\(1990\)020<0150:IMIOC>2.0.CO;2](https://doi.org/10.1175/1520-0485(1990)020<0150:IMIOC>2.0.CO;2)
- Griffies, S. M., Adcroft, A., Banks, H., Böning, C., Chassignet, E., Danabasoglu, G., et al. (2009). Problems and prospects in large-scale ocean circulation models. In J. Hall, D. E. Harrison, & D. Stammer (Eds.), *Proceedings of OceanObs'09: Sustained Ocean Observations and Information for Society* (Vol. 2, pp. 437–458). Noordwijk, The Netherlands: European Space Agency.
- Griffies, S. M., Harrison, M. J., Pacanowski, R. C., & Rosati, A. (2004). A technical guide to MOM4. GFDL Ocean Group Tech. Rep. 5, 371.
- Kantha, L. H., & Clayson, C. A. (2004). On the effect of surface gravity waves on mixing in the oceanic mixed layer. *Ocean Modelling*, *6*(2), 101–124. [https://doi.org/10.1016/S1463-5003\(02\)00062-8](https://doi.org/10.1016/S1463-5003(02)00062-8)
- Kwon, Y.-O., Alexander, M. A., Bond, N. A., Frankignoul, C., Nakamura, H., Qiu, B., & Thompson, L. A. (2010). Role of the Gulf Stream and Kuroshio-Oyashio Systems in large-scale atmosphere-ocean interaction: A review. *Journal of Climate*, *23*(12), 3249–3281. <https://doi.org/10.1175/2010jcli3343.1>
- Large, W. G., McWilliams, J. C., & Doney, S. C. (1994). Oceanic vertical mixing: A review and a model with a nonlocal boundary layer parameterization. *Reviews of Geophysics*, *32*(4), 363–403. <https://doi.org/10.1029/94RG01872>
- Large, W. G., & Yeager, S. (2009). The global climatology of an interannually varying air-sea flux data set. *Climate Dynamics*, *33*(2–3), 341–364. <https://doi.org/10.1007/s00382-008-0441-3>

- Lewis, M. R., Carr, M.-E., Feldman, G. C., Esaias, W., & McClain, C. (1990). Influence of penetrating solar radiation on the heat budget of the equatorial Pacific Ocean. *Nature*, *347*(6293), 543–545. <https://doi.org/10.1038/347543a0>
- Li, Z., Saad, Y., & Sosenkina, M. (2003). pARMS: A parallel version of the algebraic recursive multilevel solver. *Numerical Linear Algebra with Applications*, *10*(5–6), 485–509. <https://doi.org/10.1002/nla.325>
- Lin, X., Xie, S. P., Chen, X., & Xu, L. (2006). A well-mixed warm water column in the central Bohai Sea in summer: Effects of tidal and surface wave mixing. *Journal of Geophysical Research*, *111*, C11017. <https://doi.org/10.1029/2006JC003504>
- Locarnini, R., Mishonov, A., Antonov, J., Boyer, T., Garcia, H., Baranova, O., et al. (2013). In S. Levitus, A. Mishonov, & Technical Ed. (Eds.), *World Ocean Atlas 2013, volume 1: Temperature* NOAA Atlas NESDIS (Vol. 73, p. 40).
- Ma, X., Jing, Z., Chang, P., Liu, X., Montuoro, R., Small, R. J., et al. (2016). Western boundary currents regulated by interaction between ocean eddies and the atmosphere. *Nature*, *535*(7613), 533–537. <https://doi.org/10.1038/nature18640>
- Martin, P. J. (1985). Simulation of the mixed layer at OWS November and Papa with several models. *Journal of Geophysical Research*, *90*(C1), 903–916. <https://doi.org/10.1029/JC090iC01p00903>
- Mellor, G. L. (2001). One-dimensional, ocean surface layer modeling: A problem and a solution. *Journal of Physical Oceanography*, *31*(3), 790–809. [https://doi.org/10.1175/1520-0485\(2001\)031<0790:ODOSLM>2.0.CO;2](https://doi.org/10.1175/1520-0485(2001)031<0790:ODOSLM>2.0.CO;2)
- Mellor, G. L., & Yamada, T. (1982). Development of a turbulence closure model for geophysical fluid problems. *Reviews of Geophysics*, *20*(4), 851–875. <https://doi.org/10.1029/RG020i004p00851>
- Morel, A., & Antoine, D. (1994). Heating rate within the upper ocean in relation to its bio-optical state. *Journal of Physical Oceanography*, *24*(7), 1652–1665. [https://doi.org/10.1175/1520-0485\(1994\)024<1652:HRWTUO>2.0.CO;2](https://doi.org/10.1175/1520-0485(1994)024<1652:HRWTUO>2.0.CO;2)
- Pacanowski, R., & Philander, S. (1981). Parameterization of vertical mixing in numerical models of tropical oceans. *Journal of Physical Oceanography*, *11*(11), 1443–1451. [https://doi.org/10.1175/1520-0485\(1981\)011<1443:POVMIN>2.0.CO;2](https://doi.org/10.1175/1520-0485(1981)011<1443:POVMIN>2.0.CO;2)
- Qiao, F., & Huang, C. (2012). Comparison between vertical shear mixing and surface wave-induced mixing in the extratropical ocean. *Journal of Geophysical Research*, *117*, C00J16. <https://doi.org/10.1029/2012JC007930>
- Qiao, F., Yuan, Y., Ezer, T., Xia, C., Yang, Y., Lü, X., & Song, Z. (2010). A three-dimensional surface wave-ocean circulation coupled model and its initial testing. *Ocean Dynamics*, *60*(5), 1339–1355. <https://doi.org/10.1007/s10236-010-0326-y>
- Qiao, F., Yuan, Y., Yang, Y., Zheng, Q., Xia, C., & Ma, J. (2004). Wave-induced mixing in the upper ocean: Distribution and application to a global ocean circulation model. *Geophysical Research Letters*, *31*, L11303. <https://doi.org/10.1029/2004GL019824>
- Rackow, T., Goessling, H. F., Jung, T., Sidorenko, D., Semmler, T., Barbi, D., & Handorf, D. (2016). Towards multi-resolution global climate modeling with ECHAM6-FESOM. Part II: Climate variability. *Climate Dynamics*, *1–26*.
- Redi, M. H. (1982). Oceanic isopycnal mixing by coordinate rotation. *Journal of Physical Oceanography*, *12*(10), 1154–1158. [https://doi.org/10.1175/1520-0485\(1982\)012<1154:OIMBCR>2.0.CO;2](https://doi.org/10.1175/1520-0485(1982)012<1154:OIMBCR>2.0.CO;2)
- Sallée, J. B., Shuckburgh, E., Bruneau, N., Meijers, A. J., Bracegirdle, T. J., Wang, Z., & Roy, T. (2013). Assessment of Southern Ocean water mass circulation and characteristics in CMIP5 models: Historical bias and forcing response. *Journal of Geophysical Research: Oceans*, *118*, 1830–1844. <https://doi.org/10.1002/jgrc.20135>
- Scholz, P., Lohmann, G., Wang, Q., & Danilov, S. (2013). Evaluation of a Finite-Element Sea-Ice Ocean Model (FESOM) set-up to study the interannual to decadal variability in the deep-water formation rates. *Ocean Dynamics*, *63*(4), 347–370. <https://doi.org/10.1007/s10236-012-0590-0>
- Sein, D. V., Danilov, S., Biastoch, A., Durgadoo, J. V., Sidorenko, D., Harig, S., & Wang, Q. (2016). Designing variable ocean model resolution based on the observed ocean variability. *Journal of Advances in Modeling Earth Systems*, *8*, 904–916. <https://doi.org/10.1002/2016MS000650>
- Sein, D. V., Koldunov, N. V., Danilov, S., Wang, Q., Sidorenko, D., Fast, L., et al. (2017). Ocean modeling on a mesh with resolution following the local Rossby radius. *Journal of Advances in Modeling Earth Systems*, *9*, 2601–2614. <https://doi.org/10.1002/2017MS001099>
- Shu, Q., Qiao, F., Song, Z., Xia, C., & Yang, Y. (2011). Improvement of MOM4 by including surface wave-induced vertical mixing. *Ocean Modelling*, *40*(1), 42–51. <https://doi.org/10.1016/j.ocemod.2011.07.005>
- Sidorenko, D., Rackow, T., Jung, T., Semmler, T., Barbi, D., Danilov, S., et al. (2015). Towards multi-resolution global climate modeling with ECHAM6-FESOM. Part I: Model formulation and mean climate. *Climate Dynamics*, *44*(3–4), 757–780. <https://doi.org/10.1007/s00382-014-2290-6>
- Sidorenko, D., Wang, Q., Danilov, S., & Schröter, J. (2011). FESOM under coordinated ocean-ice reference experiment forcing. *Ocean Dynamics*, *61*(7), 881–890. <https://doi.org/10.1007/s10236-011-0406-7>
- Siegel, D. A., Ohlmann, J. C., Washburn, L., Bidigare, R. R., Nosse, C. T., Fields, E., & Zhou, Y. (1995). Solar radiation, phytoplankton pigments and the radiant heating of the equatorial Pacific warm pool. *Journal of Geophysical Research*, *100*(C3), 4885–4891. <https://doi.org/10.1029/94JC03128>
- Song, Y., Qiao, F., & Song, Z. (2012a). Improved simulation of the South Asian summer monsoon in a coupled GCM with a more realistic ocean mixed layer. *Journal of the Atmospheric Sciences*, *69*(5), 1681–1690. <https://doi.org/10.1175/JAS-D-11-0235.1>
- Song, Z., Qiao, F., & Song, Y. (2012b). Response of the equatorial basin-wide SST to non-breaking surface wave-induced mixing in a climate model: An amendment to tropical bias. *Journal of Geophysical Research*, *117*, C00J26. <https://doi.org/10.1029/2012JC007931>
- Steele, M., Morley, R., & Ermold, W. (2001). PHC: A global ocean hydrography with a high-quality Arctic Ocean. *Journal of Climate*, *14*(9), 2079–2087. [https://doi.org/10.1175/1520-0442\(2001\)014<2079:PAGOHW>2.0.CO;2](https://doi.org/10.1175/1520-0442(2001)014<2079:PAGOHW>2.0.CO;2)
- Sweeney, C., Gnanadesikan, A., Griffies, S. M., Harrison, M. J., Rosati, A. J., & Samuels, B. L. (2005). Impacts of shortwave penetration depth on large-scale ocean circulation and heat transport. *Journal of Physical Oceanography*, *35*(6), 1103–1119. <https://doi.org/10.1175/JPO2740.1>
- Timmermann, R., Wang, Q., & Hellmer, H. (2012). Ice-shelf basal melting in a global finite-element sea-ice/ice-shelf/ocean model. *Annals of Glaciology*, *53*(60), 303–314. <https://doi.org/10.3189/2012AoG60A156>
- Wang, C., Zhang, L., Lee, S.-K., Wu, L., & Mechoso, C. R. (2014). A global perspective on CMIP5 climate model biases. *Nature Climate Change*, *4*(3), 201–205. <https://doi.org/10.1038/nclimate2118>
- Wang, Q., Danilov, S., Fahrback, E., Schröter, J., & Jung, T. (2012). On the impact of wind forcing on the seasonal variability of Weddell Sea bottom water transport. *Geophysical Research Letters*, *39*, L06603. <https://doi.org/10.1029/2012GL051198>
- Wang, Q., Danilov, S., Jung, T., Kaleschke, L., & Wernecke, A. (2016). Sea ice leads in the Arctic Ocean: Model assessment, interannual variability and trends. *Geophysical Research Letters*, *43*, 7019–7027. <https://doi.org/10.1002/2016GL068696>
- Wang, Q., Danilov, S., & Schröter, J. (2008). Finite element ocean circulation model based on triangular prismatic elements, with application in studying the effect of topography representation. *Journal of Geophysical Research*, *113*, C05015. <https://doi.org/10.1029/2007JC004482>

- Wang, Q., Danilov, S., Sidorenko, D., Timmermann, R., Wekerle, C., Wang, X., et al. (2014). The Finite Element Sea Ice-Ocean Model (FESOM) v.1.4: Formulation of an ocean general circulation model. *Geoscientific Model Development*, 7(2), 663–693. <https://doi.org/10.5194/gmd-7-663-2014>
- Wang, Q., Ilicak, M., Gerdes, R., Drange, H., Aksenov, Y., Bailey, D. A., et al. (2016). An assessment of the Arctic Ocean in a suite of interannual CORE-II simulations. Part II: Liquid freshwater. *Ocean Modelling*, 99, 86–109. <https://doi.org/10.1016/j.ocemod.2015.12.009>
- Wang, Q., Wekerle, C., Danilov, S., Wang, X., & Jung, T. (2018). A 4.5 km resolution Arctic Ocean simulation with the global multi-resolution model FESOM 1.4. *Geoscientific Model Development*, 11(4), 1229.
- Wang, Y., Qiao, F., Fang, G., & Wei, Z. (2010). Application of wave-induced vertical mixing to the K profile parameterization scheme. *Journal of Geophysical Research*, 115, C09014. <https://doi.org/10.1029/2009JC005856>
- Wekerle, C., Wang, Q., Danilov, S., Jung, T., & Schröter, J. (2013). The Canadian Arctic Archipelago throughflow in a multiresolution global model: Model assessment and the driving mechanism of interannual variability. *Journal of Geophysical Research: Oceans*, 118, 4525–4541. <https://doi.org/10.1002/jgrc.20330>
- Wekerle, C., Wang, Q., Danilov, S., Schourup-Kristensen, V., von Appen, W. J., & Jung, T. (2017). Atlantic Water in the Nordic Seas: Locally eddy-permitting ocean simulation in a global setup. *Journal of Geophysical Research: Oceans*, 122, 914–940. <https://doi.org/10.1002/2016JC012121>
- Wekerle, C., Wang, Q., von Appen, W. J., Danilov, S., Schourup-Kristensen, V., & Jung, T. (2017). Eddy-resolving simulation of the Atlantic Water Circulation in the Fram Strait with focus on the seasonal cycle. *Journal of Geophysical Research: Oceans*, 122, 8385–8405. <https://doi.org/10.1002/2017JC012974>
- White, L., Deleersnijder, E., & Legat, V. (2008). A three-dimensional unstructured mesh finite element shallow-water model, with application to the flows around an island and in a wind-driven, elongated basin. *Ocean Modelling*, 22(1–2), 26–47. <https://doi.org/10.1016/j.ocemod.2008.01.001>